Superlattices of Bi₂Se₃/In₂Se₃: Growth characteristics and structural properties

Z. Y. Wang,[1] X. Guo,[1] H. D. Li,[1,2] T. L. Wong,[3] N. Wang,[3] and M. H. Xie[1,a]

[1]*Physics Department, The University of Hong Kong, Pokfulam Road, Hong Kong*
[2]*Department of Physics, Beijing Jiaotong University, Beijing 100044, China*
[3]*Physics Department, Hong Kong University of Science and Technology, Clear Water Bay, Kowloon, Hong Kong*

Superlattices (SLs) consisted of alternating Bi₂Se₃ and In₂Se₃ layers are grown on Si(111) by molecular-beam epitaxy. Bi₂Se₃, a three-dimensional topological insulator (TI), showed good chemical and structural compatibility with In₂Se₃, a normal band insulator with large energy bandgap. The individual layers in the SLs are very uniform, and the hetero-interfaces are sharp. Therefore, such SL structures are potential candidates for explorations of the quantum size effects of TIs. © 2011 American Institute of Physics. [doi:10.1063/1.3610971]

Along with the extensive researches of materials and properties of three-dimensional (3D) topological insulators (TIs),[1] attention has increasingly been paid on ultrathin films and nanostructures of such materials for enhanced effects and properties associated with the topological states of electrons.[2] In the same line of thoughts, multi-layered structures constituted of TIs and normal band insulators, such as superlattices (SLs) or multiple quantum wells (MQWs) of… Bi₂Se₃/ZnSe…, have been attempted by the technique of molecular-beam epitaxy (MBE).[3] Since SLs and MQWs can be used for future device applications, growth of high quality SL or MQW samples is of great fundamental and practical importance. Unfortunately, the combination of topological insulator Bi₂Se₃ and normal band insulator ZnSe does not lead to desired heterostructures with good structural quality.[3]

In this letter, we report growth of…Bi₂Se₃/In₂Se₃… SL structures with great structural quality. The interfaces of Bi₂Se₃/In₂Se₃ and In₂Se₃/Bi₂Se₃ are symmetrical and sharp. Transmission electron microscopy (TEM) examinations of the samples reveal few defects, indicating strain relaxation is at the van der Waals gaps of the hetero-interfaces. X-ray diffraction (XRD) measurements show satellite peaks characteristic of the SL structure of the samples, suggesting good uniformity of the individual layers.

The compound of In₂Se₃ is a well known semiconductor (insulator) that has an energy bandgap of 1.2-1.3 eV.[4,5] It is conveniently grown in MBE reactors designated for Bi₂Se₃ growth, as both are selenide compounds showing similar growth conditions. In₂Se₃ is also a layered material as of Bi₂Se₃, yet it has a relatively small lattice mismatch with Bi₂Se₃ ($\sim$3.4%). Therefore, the two are chemically and structurally compatible, suitable for growth of SL or MQW structures.

Growth and surface characterizations of the heterostructures are made in a customized MBE system, where indium (In), bismuth (Bi), and selenium (Se) fluxes are generated from Knudsen cells.[6] In situ reflection high energy electron diffraction (RHEED) is employed to monitor the growing surfaces in real-time to assess the film growth mode, lattice misfit strain, and surface reconstructions. The RHEED specular-beam intensity is recorded, and from its oscillations, we obtain the deposition rates of the films.[6] Room temperature (RT) scanning tunneling microscopy (STM) is used to examine the morphologies of the grown samples, where the tunneling current is 0.2 nA and the sample bias is −0.45 V. The substrates are nominally flat Si(111), which are deoxidized at $\geq$1000 °C in vacuum for clear (7 × 7) surfaces. Afterwards, we prepare a thin InSe buffer on Si(111)-(7 × 7) by depositing 3 monolayers In at $\sim$220 K followed by annealing in a flux of Se at 490 K until a set of $(\sqrt{3} \times \sqrt{3})R30°$ pattern appears in the RHEED. The distance between the diffraction streaks is found to correspond well with the lattice parameter of α-phase In₂Se₃. Some previous studies showed the $(\sqrt{3} \times \sqrt{3})R30°$ structures only for γ-phase In₂Se₃.[5,7] However, the latter has a lattice parameter ($\sim$ 4.26 Å) that is far larger than that measured by the RHEED. Therefore, we tend to believe the buffer is of α-phase In₂Se₃.

Bi₂Se₃ deposition on In₂Se₃ buffer is conducted at 180 °C using a Bi to Se flux ratio of 1:10. From the persistence of the streaky RHEED patterns, we infer that two-dimensional (2D) layer-by-layer growth mode of Bi₂Se₃ is achieved. Indeed, the RHEED intensity starts to oscillate upon the initiation of Bi₂Se₃ deposition [Fig. 1 inset (i)]. A sample containing a thin layer of Bi₂Se₃ (9 nm) deposited on such In₂Se₃ buffer is characterized by XRD, and the result of θ - 2θ scan is shown in Fig. 1. It reveals not only the diffraction peaks of the substrate (Si) and Bi₂Se₃ epifilm but also Kiessig fringes with the period corresponding well with the film thickness, implying good film uniformity and sharp interfaces. No In₂Se₃-related peak is seen in the XRD data, probably because the buffer is too thin or they overlap those of Bi₂Se₃. The inset (ii) in Fig. 1 presents a STM image of the surface after about 1.5 quintuple layers (QLs) Bi₂Se₃ deposition on In₂Se₃ buffer, revealing an atomically flat surface with 1 QL high nucleation islands. Here, we would like to comment that such Bi₂Se₃ films grown on In₂Se₃ buffers appear superior to those grown on the amorphous buffers reported earlier.[3,6] They show similarly good surfaces and electrical properties, if not better, but also improved film

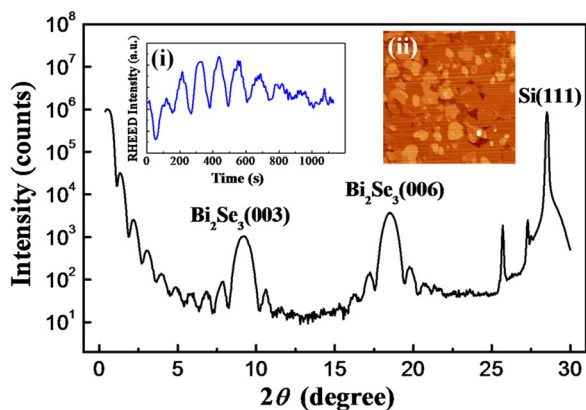a)Author to whom correspondence should be addressed. Electronic mail: mhxie@hku.hk.

FIG. 1. (Color online) XRD θ-2θ scan of a 9 nm thick Bi_2Se_3 film on In_2Se_3 buffer grown on Si(111). Inset (i): RHEED intensity oscillation during the initial stage Bi_2Se_3 deposition. Inset (ii) STM image (size: 300×300 nm^2) of the surface of a thin ($\sim$1.5 QLs) Bi_2Se_3 film deposited on In_2Se_3 buffer.

adherence to the substrate for easier device processing. A comparison of Bi_2Se_3 grown on different buffers and substrates is summarized in a different publication,[8] and in the following, we focus on the heteroepitaxy of In_2Se_3 on Bi_2Se_3 and of Bi_2Se_3 on In_2Se_3 for growth of superlattice structures.

Depositions of In_2Se_3 on Bi_2Se_3 and Bi_2Se_3 on In_2Se_3 are readily achieved by switching In and Bi fluxes while keeping the flux of Se unchanged. For the purpose of In_2Se_3 growth, the In source has been set at a similar flux to Bi, i.e., In:Se $\sim$ Bi:Se $\sim$ 1:10. Fig. 2(a) depicts the RHEED specular-beam intensity variation during deposition of the SL structure of alternating Bi_2Se_3 and In_2Se_3, while typical RHEED patterns of the respective surfaces are shown in the insets. Note that during the first Bi_2Se_3 layer deposition on In_2Se_3 buffer, the RHEED intensity oscillates as mentioned earlier, but such oscillations disappear later due to a change of the growth mode from island nucleation to step-flow. It is also seen that at the start of In_2Se_3 deposition on Bi_2Se_3, the RHEED intensity drops suddenly, which may reflect a roughening of the surface. Indeed, a slightly rougher surface of In_2Se_3 than that of Bi_2Se_3 may be inferred from a thickening and elongation of the diffraction streaks in inset (ii) than (i) of Fig. 2, which are RHEED patterns taken from In_2Se_3 and Bi_2Se_3 layers, respectively. However, we also wish to point out that the specular spot of the RHEED is in the vicinity of the (009) Bragg spot of bulk Bi_2Se_3; therefore a lattice parameter change upon In_2Se_3 deposition makes the specular-beam off the Bragg spot, contributing further to the intensity drop. Similarly, upon the commencement of Bi_2Se_3 growth on In_2Se_3, there is a sharp intensity rise, part of which is due to the smoothening of the surface and another part is due to a shift of the Bragg spot relative to the specular beam. Regardless of the intensity variations, the RHEED pattern remains streaky showing an unstructured (1×1) pattern throughout the deposition process. Therefore, 2D layer-by-layer growth is maintained. This contrasts to the case of Bi_2Se_3/ZnSe growth, where there is a tendency of 3D islanding of ZnSe surface when deposited on Bi_2Se_3.[3] This fact reflects the very nature of van der Waals bonding at the Bi_2Se_3/In_2Se_3 hetero-interfaces. They are of low surface energy, and the lattice misfit strains are easily relieved without breaking chemical bonds.

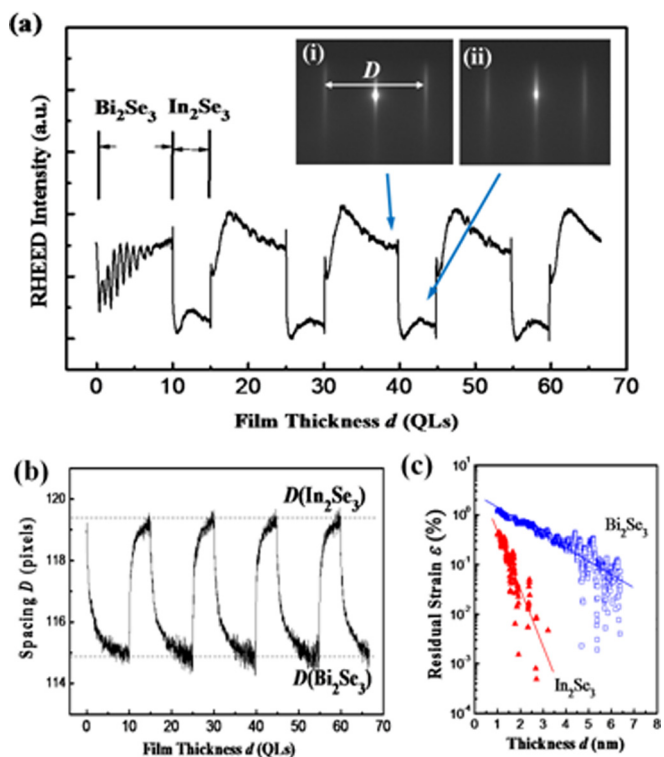FIG. 2. (Color online) Evolution of (a) the RHEED specular-beam intensity and (b) the inter-streak spacing (D) during deposition of the Bi_2Se_3/In_2Se_3 superlattice structure. The inset (i) and (ii) in (a) show the RHEED patterns taken from the growing Bi_2Se_3 and In_2Se_3 surfaces, respectively. The two dashed-dotted lines in (b) represent the D values of strain-free Bi_2Se_3 and In_2Se_3 films obtained from very thick ($>$100 nm) layers. (c) Derived residual strain ϵ from the experimental D, showing the exponential strain-relaxation processes. The thin lines represent results of the least-square fitting of the data.

Strain states of the heterostructures during the SL sample growth are monitored by the RHEED as well. The evolution of the measured reciprocal lattice parameter D [defined in the inset (i) of Fig. 2(a)] is shown in Fig. 2(b). First, one observes the lattices of heteroepitaxial Bi_2Se_3 and In_2Se_3 approach their strain-free parameters with increasing deposition thicknesses. A closer look at the strain relaxation processes [Fig. 2(c)] reveals that the residual strain defined as $\varepsilon = (a-a_0)/a_0 = (D_0-D)/D$ follows an exponential relation with time or layer thickness, h, i.e., $\varepsilon = \varepsilon_0 \exp(-h/\lambda)$,[9,10] where a and D are, respectively, real- and reciprocal-space lattice parameters of the epifilm, while a_0 and D_0 are the corresponding parameters for a strain-free layer. ε_0 is the lattice misfit between the epifilm and the substrate, and for Bi_2Se_3/In_2Se_3, it is $\sim$3.4% as mentioned earlier. The constant λ characterizes the rate at which strain relaxes (i.e., the thickness at which strain is reduced by a factor of $e \approx 2.718$). Least-square fittings of the data in Fig. 2(c) result in $\lambda \sim 16$ Å and ~ 4 Å, respectively, for the processes of Bi_2Se_3 deposition on In_2Se_3 and In_2Se_3 growth on Bi_2Se_3. These are relatively small values (i.e., $\leq 1 \sim 2$ QLs), characterizing a fast rate of strain relaxation process. According to elasticity theory, there would exist a critical film thickness h_c, below which a coherent film can be grown without strain-relaxation.[11] If so, for a lattice misfit of $\sim$3.4% as in Bi_2Se_3/In_2Se_3, $h_c \sim 20$ Å, assuming the strain-relieving dislocations to have the Burgers vector of ~ 0.4 nm in magnitude. This is not what is observed by experiments. Instead, one finds the
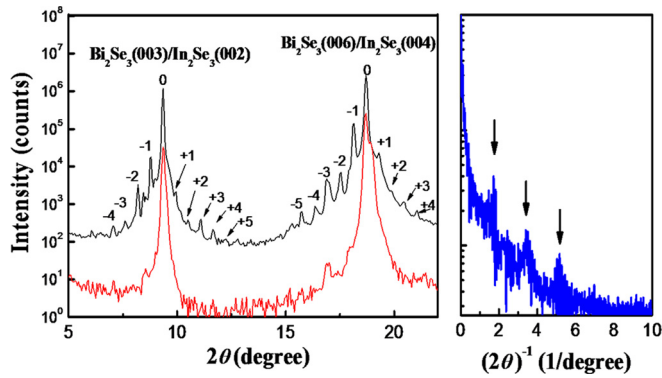
FIG. 3. (Color online) (a) XRD θ-2θ scans of a 5 nm-In_2Se_3/10 nm-Bi_2Se_3 SL sample (top) and a single-layered heterostructure of Bi_2Se_3/In_2Se_3 (bottom). (b) FFT of the XRD data of the SL sample, where the downward arrows point to peaks corresponding to the periodicity of the satellite peaks seen in the θ-2θ scan. Such peaks or the periodicity of the satellites translate into a SL structure with 15 nm thickness period.

FIG. 4. TEM micrograph showing the alternating 3 nm-In_2Se_3/7 nm-Bi_2Se_3 layers in a SL sample. Inset: Transmission electron diffraction data of the same sample.

strain to relax at the very start of the heteroepitaxy. Together with the small λ derived above, it asserts a strain relaxation process occurring at the van der Waals interfaces, where Bi_2Se_3 and In_2Se_3 compounds couple very weakly. Strain relaxation invokes no chemical bond breaking. On the other hand, the fact that strain does not fully relax upon the commencement of hetero-growth indicates some extents of constraints of the lattice by that of the substrate at the van der Waals interface. This conforms to the very nature of van der Waals epitaxy.[6,12]

Lastly in Fig. 2, we observe the surfaces and strain states to evolve highly repeatedly during different periods of… In_2Se_3/Bi_2Se_3… SL growth. It implies high uniformity of the structures. To show this, we present, in Fig. 3(a), a XRD θ-2θ scan of a 20-period…5 nm-In_2Se_3/10 nm-Bi_2Se_3… SL sample. For comparison, result from a single-layered heterostructure of In_2Se_3/Bi_2Se_3 is also shown. As is seen, up to five satellite peaks are detected from the SL sample, confirming the integrity of the structure. From the period of the satellite peaks as well as from its FFT result [Fig. 3(b)], we derive the period of the SL structure to be of 15 nm, matching exactly with the designed thickness period of the SL structure. Fig. 4 shows a high-resolution TEM micrograph of a similar sample, i.e., 3 nm-In_2Se_3/7 nm-Bi_2Se_3 SL, from which alternating In_2Se_3/Bi_2Se_3 layers are clearly resolvable. The hetero-interfaces are sharp. No extended defect is seen. However, there appear some slight contrast variations, particularly in the regions of In_2Se_3 layers. This may be caused by a residual strain field in the film. The presence of minute amount of residual strain in In_2Se_3 layers may be inferred from Fig. 2(b), in which we observe the lattice constant of the In_2Se_3 layer does not reach its strain-free value at the thickness of 3 nm. From the electron diffraction pattern shown in the inset of Fig. 4, we observe only diffraction spots from Bi_2Se_3 and In_2Se_3 crystals (overlapped to each other), suggesting high crystallinity of the phases in the materials.

To conclude, Bi_2Se_3 and In_2Se_3 form a superior combination for heteroepitaxy of SL and/or MQW structures, where topological insulator is embedded in a normal band insulator for exploration of quantum size and surface-coupling effects. The van der Waals hetero-interface ensures the 2D gro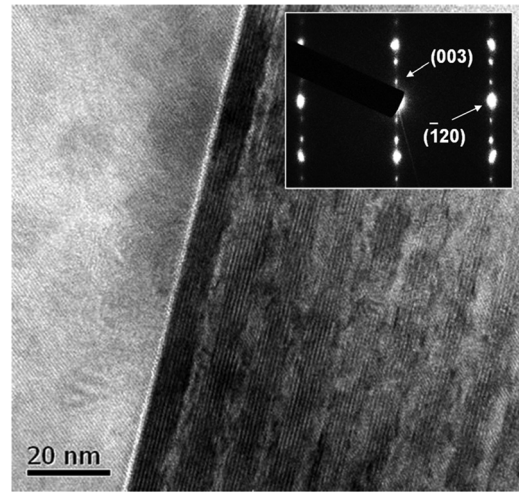wth mode of the structure with sharp interfaces. Strain relaxation is realized at the van der Waals gaps without invoking dislocations. The SL of In_2Se_3/Bi_2Se_3 fabricated by MBE show high structural quality, which are candidates for future transport and optical studies.

[1]Y. Xia, D. Qian, D. Hsieh, L. Wray, A. Pal, H. Lin, A. Bansil, D. Grauer, Y. S. Hor, R. J. Cava, and M. Z. Hasan, Nat. Phys. **5**, 398 (2009); H. J. Zhang, C. X. Liu, X. L. Qi, X. Dai, Z. Fang, and S. C. Zhang, Nat. Phys. **5**, 438 (2009).
[2]Y. Zhang, K. He, C. Z. Chang, C. L. Song, L. L. Wang, X. Chen, J. F. Jia, Z. Fang, X. Dai, W. Y. Shan, S. Q. Shen, Q. Niu, X. L. Qi, S. C. Zhang, X. C. Ma, and Q. K. Xue, Nat. Phys. **6**, 584 (2010); H. L. Peng, K. J. Lai, D. S. Kong, S. Meister, Y. L. Chen, X. L. Qi, S. C. Zhang, Z. X. Shen, and Y. Cui, Nat. Mater. **9**, 225 (2010); G. Wang, X. Zhu, J. Wen, X. Chen, K. He, L. Wang, X. Ma, Y. Liu, X. Dai, Z. Fang, J. Jia, and Q. Xue, Nano. Res. **3**, 874 (2010); G. H. Zhang, H. J. Qin, J. Teng, J. D. Guo, Q. L. Guo, X. Dai, Z. Fang, and K. H. Wu, Appl. Phys. Lett. **95**, 053114 (2009); Y. Y. Li, G. A. Wang, X. G. Zhu, M. H. Liu, C. Ye, X. Chen, Y. Y. Wang, K. He, L. L. Wang, X. C. Ma, H. J. Zhang, X. Dai, Z. Fang, X. C. Xie, Y. Liu, X. L. Qi, S. C. Zhang, J. F. Jia, and Q. K. Xue, Adv. Mater. **22**, 4002 (2010).
[3]H. D. Li, Z. Y. Wang, X. Guo, T. L. Wong, N. Wang, and M. H. Xie, Appl. Phys. Lett. **98**, 043104 (2011).
[4]M. Emziane, S. Marsillac, and J. C. Bernede, Mater. Chem. Phys. **62**, 84 (2000).
[5]J. P. Ye, S. Soeda, Y. Nakamura, and O. Nittono, Jpn. J. Appl. Phys., Part 1 **37**, 4264 (1998).
[6]H. D. Li, Z. Y. Wang, X. Kan, X. Guo, H. T. He, Z. Wang, J. N. Wang, T. L. Wong, N. Wang, and M. H. Xie, New J. Phys. **12**, 103038 (2010).
[7]C. Y. Lu, P. J. Shamberger, E. N. Yitamben, K. M. Beck, A. G. Joly, M. A. Olmstead, and F. S. Ohuchi, Appl. Phys. A **93**, 93 (2008).
[8]Z. Y. Wang, X. Guo, H. D. Li, W. K. Ho, and M. H. Xie, "Growth characteristics of topological insulator Bi_2Se_3 films on different substrates" (unpublished).
[9]G. Feuillet, B. Daudin, F. Widmann, J. L. Rouviere, and M. Arlery, J. Cryst. Growth **190**, 142 (1998).
[10]A. Bourret, C. Adelmann, B. Daudin, J. L. Rouviere, G. Feuillet, and G. Mula, Phys. Rev. B **63**, 245307 (2001).
[11]J. W. Matthews and A. E. Blakeslee, J. Cryst. Growth **27**, 118 (1974).
[12]A. Koma, Thin Solid Films **216**, 72 (1992); A. Koma, Surf. Sci. **267**, 29 (1992).